

Optimization of Chinese solar greenhouse building parameters based on CFD simulation and entropy weight method

Fen He^{1,2}, Changqing Si³, Xiaoming Ding^{1,2}, Zhenjun Gao⁴, Binbin Gong⁵, Fei Qi^{1,2*}, Yilei Yin^{1,2}, Qian Feng^{1,2}

(1. Academy of Agricultural Planning and Engineering, Ministry of Agriculture and Rural Affairs, Beijing 100125, China;

2. Key Laboratory of Farm Building in Structure and Intelligent Construction, Ministry of Agriculture and Rural Affairs, Beijing 100125, China;

3. Shenzhen Envicool Technology Co. Ltd., Shenzhen 518129, China;

4. College of Mechanical & Power Engineering, China Three Gorges University, Yichang 443002, Hubei, China;

5. Hebei Agricultural University, Baoding 071001, Hebei, China)

Abstract: The building parameters of Chinese solar greenhouse (CSG) directly affect the front roof lighting and indoor thermal environment. In order to obtain the optimal parameter combination, a building parameter optimization method based on computational fluid dynamics (CFD) simulation and entropy weight method was proposed. Firstly, a three-dimensional thermal and humidity environment model of CSG was constructed considering the coupling effect of soil, crop, and back wall based on CFD. The reliability of the model was validated through experiments in a CSG of Yongqiang County, Hebei Province of China. Then, the indoor air temperature rise rate, air temperature and humidity uneven coefficient, and average air temperature and humidity were selected as the evaluation indicators of CSG thermal and humidity environment. The ridge height, back wall height and the horizontal projection of back roof of CSG were selected as the three factors of the orthogonal test plan, and a three-factor and four-level plan was designed, resulting in 16 different parameter combinations. By use of CFD simulation, the thermal and humidity environment evaluation indicators under different parameter combinations were calculated. The entropy weight method was used to assign weights to the evaluation indicators, and the comprehensive evaluation indicators of CSG thermal and humidity environment were obtained based on the linear weighting principle. By comparing comprehensive evaluation indicators, the optimal combination of building parameters was obtained with a ridge height of 5.72 m, a back wall height of 3.2 m, and a horizontal projection of 2.1 m on the back roof. The research results can provide a practical and feasible method for optimizing the building parameters of CSG, and provided theoretical guidance for the structural design and optimization of CSG.

Keywords: CSG, thermal and humidity environment, CFD simulation, entropy weight method, building parameter optimization

DOI: [10.25165/j.ijabe.20231606.8331](https://doi.org/10.25165/j.ijabe.20231606.8331)

Citation: He F, Si C Q, Ding X M, Gao Z J, Gong B B, Qi F, et al. Optimization of Chinese solar greenhouse building parameters based on CFD simulation and entropy weight method. Int J Agric & Biol Eng, 2023; 16(6): 48–55.

1 Introduction

Chinese solar greenhouse (CSG) is a unique type of greenhouse, which can achieve overwintering production of fruits and vegetables in northern China without auxiliary heating^[1,2]. According to the 2022 national agricultural mechanization statistical annual report, as of the end of 2022, the total area of CSG has reached 520 000 hm², accounting for nearly 30% of China's greenhouse area. CSG were mainly distributed in Huang-Huai-Hai,

northeast and northwest China, accounting for more than 80% of the total CSG area^[3]. As an important way to solve the stable supply of winter vegetable in northern China, it has played an important role in ensuring supply and promoting income growth^[4].

CSG is mainly composed of an enclosure structure (back wall, gable), front and back roof, support framework (bamboo, wood, cement, steel skeleton, etc.). The front roof is covered with insulation quilts, and is equipped with rolling shutter machines and other equipments. During the day, the insulation quilt is rolled up, and solar radiation enters into the greenhouse from the transparent front roof. The indoor air temperature gradually increases, and the back wall and soil with good heat storage performance absorb the accumulated heat of solar radiation. At night, the insulation quilt is put down, and the back wall and soil release heat to maintain indoor temperature and ensure crop growth normally. It can be seen that solar radiation is the main energy source and the important factor affecting the light and thermal environment of CSG. To achieve maximum solar radiation in a CSG, ensure crop photosynthesis, and increase indoor temperature, it is necessary to take reasonable values for CSG building parameters^[5].

Received date: 2023-05-09 Accepted date: 2023-09-26

Biographies: Fen He, PhD, research interest: greenhouse environment engineering, Email: hufen_2005@163.com; Changqing Si, MS, research interest: greenhouse environment simulation, Email: 1061070924@qq.com; Xiaoming Ding, MS, research interest: protected cultivation, Email: 32105255@qq.com; Zhenjun Gao, PhD, research interest: greenhouse environment simulation, Email: 570186276@qq.com; Binbin Gong, MS, research interest: greenhouse environment engineering, Email: yygb@hebau.edu.cn; Yilei Yin, MS, research interests: protected cultivation, Email: 276089613@qq.com; Qian Feng, MS, research interest: protected cultivation, Email: 3250772735@qq.com.

*Corresponding author: Fei Qi, Professor, research interest: agricultural engineering. Academy of Agricultural Planning and Engineering, Ministry of Agriculture and Rural Affairs, Beijing 100125, China. Tel: +86-13901216776, Email: qf2008@188.com.

In recent years, researchers have placed more emphasis on combining building parameters and considering the crops

themselves in CSG design. In Chinese agricultural industry standard “Code for design of Chinese solar greenhouse”, in order for plants to receive as much solar radiation as possible, when determining the main dimensions of CSG, it was proposed to ensure that during the winter solstice production period, at least 4 hours before and after noon (10:00-14:00), the incident angle between direct sunlight and the plane formed by the connection between the front foot of the greenhouse and the roof ridge should not exceed 43° ^[6]. Cao et al.^[7] used the minimum outdoor temperature below 0°C to ensure that at least a portion of the back wall can receive direct sunlight within 4 hours before and after noon (10:00-14:00) as the control condition, and provided a reasonable time period for the back wall of a CSG to receive direct sunlight in different latitude areas. The calculation method for the horizontal projection length of the back roof and the height of the back wall of the CSG was obtained. The sliding roof CSG designed by Tong et al.^[8] moved the roof ridge forward and increased the lighting roof angle by 15° . In winter, the average daylight efficiency increased by 15.4% compared to ordinary CSG, and the solar interception increased by 11.6%. Yang et al.^[9] proposed that the height span ratio of CSG in the same region is not affected by span change, but only related to the change of local outdoor air temperature and solar radiant intensity. Combining Energy Plus energy consumption simulation software, and applying single variable control method, the appropriate height span ratio of CSG buildings in different geographical latitudes with span of 6-12 m was calculated. Zhang et al.^[2] proposed a model for optimizing the structural dimensions of CSG based on canopy height. The model sets three constraint conditions for crop lighting, greenhouse heat storage, and insulation requirements. Through the model, the building dimensions of CSG in different regions can be calculated and the cost can be optimized.

With the rapid development of CFD technology, it is widely used in greenhouse thermal environment simulation and natural ventilation simulation^[10-12]. Researchers have also applied it to simulate the thermal and humidity environment of CSG and the impact of different building parameter values on the environment^[13-15]. Wu et al.^[16] introduced the concept of ridge position ratio ($\text{RPR}=\text{back roof projection length/span}$) and constructed a CFD model to determine the impact of position ratio values from 0.1 to 0.45 on indoor light and thermal environment. Tong et al.^[17] constructed a CSG model with different combinations of span and ridge height, and analyzed the effects of greenhouse building parameters on heat loss, heat gain, and temperature. Li et al.^[18] introduced wall to slope ratio (ratio of back wall height to back roof length), spinal position ratio (ratio of back roof projection length to

span), and ridge to span ratio (ratio of ridge to span) to simulate the temperature field of greenhouse with different design parameters by using a CFD model. It was analyzed that changes in ridge to span ratio led to more significant changes in indoor light and thermal environment compared to wall to slope ratio and spinal position ratio, and it was considered that a value of 0.68 was more reasonable.

This study innovatively proposed a parameter optimization method for CSG buildings based on CFD simulation and entropy weight method. This method was based on CFD to construct a thermal and humidity environment model for a CSG, and the reliability of the model was verified through practical testing. Calculate the thermal and humidity environment evaluation indicators under different parameter combinations based on this model. The entropy weight method was used to assign weights to the evaluation indicators and obtain comprehensive evaluation indicators for the greenhouse thermal and humidity environment. By calculating and comparing the comprehensive evaluation index values, the optimal combination of building parameters can be obtained.

2 Materials and methods

2.1 Experimental greenhouse description and data collection

The experimental greenhouse located in Yongqing County, Hebei Province of China ($39.32^\circ\text{N}, 116.49^\circ\text{E}$, 11 m altitude). Figure 1 is the schematic diagram of experimental greenhouse, which faced south, with a length of 60 m, a span of 10 m and a ridge height of 5.32 m. And the back wall was 4 m high and 920 mm thick. From inside to outside, it was 820 mm thick steel frame system prefabricated reinforced concrete slab fabricated wall and 100 mm thick extruded polystyrene board. The fabricated wall was a steel frame, the inner and outer layers were 80 mm thick precast concrete slabs, and the middle was 660 mm thick compacted soil, which needed to be compacted in several times. The gable was 370 mm thick shale brick with 100 mm thick extruded polystyrene board outside. The film of front roof was polyolefin film with a thickness of 0.12 mm. The front bottom of greenhouse adopted electric film rolling ventilation, and the ridge adopted intelligent roof ventilation system to adjust the size of air outlet according to the inside air temperature feedback. The front roof was covered with composite insulation quilt, and the time of rolling up and putting down was 8:30-9:00 and 16:00-16:30 respectively. The air heating system was not installed in the greenhouse. Tomatoes were cultivated in substrate bags. The surface of the whole planting area was covered with black film mulching and the crop irrigation method was drip irrigation with water and fertilizer integration.

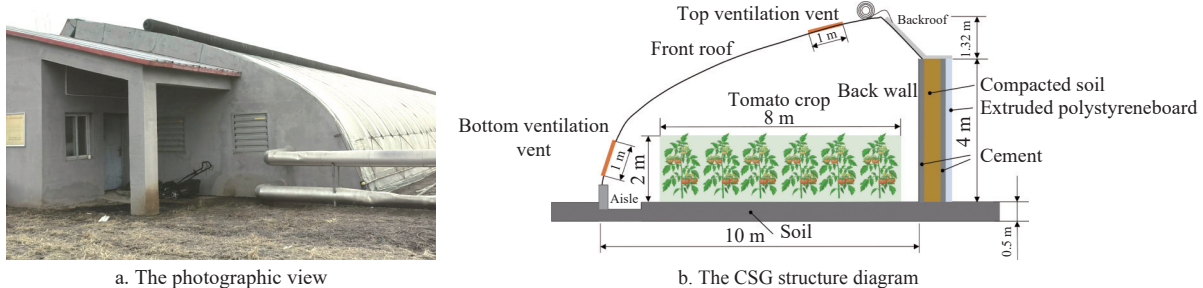


Figure 1 Overview of experimental greenhouse

The experiment was carried out in October 2021 to April 2022. The testing parameters mainly included indoor and outdoor environmental parameters. Outdoor environmental parameters

included outdoor air temperature, relative humidity, solar radiation, wind speed, etc., which were measured by HortiMaX meteorological station. Indoor environmental parameters included

air temperature, relative humidity, soil temperature, back wall temperature, solar radiation. The air temperature and relative humidity were collected by temperature and humidity recorder (HOBO UX100-003, Onset, USA). To avoid environmental factors such as solar radiation affecting the accuracy of temperature and humidity sensor measurement, aluminum foil was used to cover the outside of recorder. The soil temperature and back wall temperature were measured using copper constantan thermocouples and saved to a data collector (CR1000, Campbell Scientific Inc., USA). The indoor solar radiant intensity was collected by solar radiation sensor (S-LiB-M003, Onset, USA) and saved to the HOBO H21-USB 5-

channel small weather station. The data collection time interval was 10 min. The layout of measuring points is shown in Figure 2.

2.2 Computer simulation

2.2.1 Physical model

Using the experimental greenhouse as a physical prototype, the geometric computational domain of model is shown in Figure 3. Indoor and outdoor air was defined as a fluid domain, crop areas were defined as porous media, and the rest were defined as solid areas. At the same time, the marginal soil on the north and south sides was considered in the model. The main material physical parameters in the CSG are listed in Table 1.

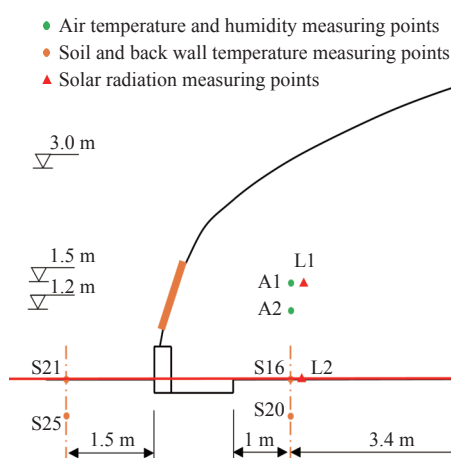


Figure 2 Measuring points arrangement

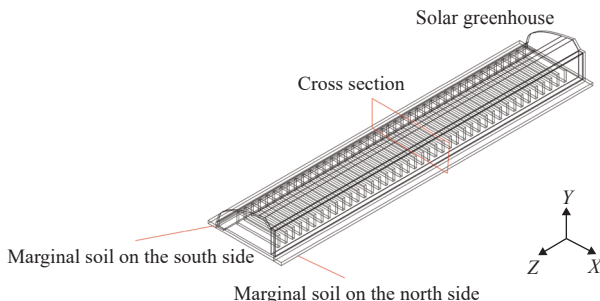


Figure 3 Geometric computational domain of model

Table 1 Physical parameters of main materials in CSG

| Materials | Density/ kg·m ⁻³ | Specific heat/ (J·kg ⁻¹ ·K ⁻¹) | Thermal conductivity/ (W·m ⁻¹ ·K ⁻¹) |
|----------------------------|--------------------------------|--|--|
| PO film | 950 | 1600 | 0.19 |
| Gable | 1600 | 1050 | 1.432 |
| Soil | 1600 | 2200 | 0.80 |
| Tomato crop | 560 | 2100 | 0.19 |
| Air | 1.225 | 1006.7 | 0.0240 |
| Extruded polystyrene board | 32 | 1500 | 0.028 |
| Insulation quilt | 150 | 1880 | 0.06 |
| Cement | 2300 | 920 | 1.51 |

A closed greenhouse during the day on a sunny winter day was chosen as the typical working condition, the testing time was on February 22, 2022, and the minimum outdoor temperature was 8.8°C. Due to the closed state of greenhouse, the outdoor air was not considered in the model. The external environment was fitted as a time-varying equation and loaded onto the outer surface of the greenhouse enclosure structure as a boundary condition using user defined functions (UDF) method.

The model adopted structured and unstructured grid partitioning, and performed grid refinement on areas with high gradients. The maximum grid size of the model was 850 mm, the overall average mass of the grid was greater than 0.82, the average skewness was less than 0.24, and the minimum orthogonal mass was greater than 0.1, meeting the quality requirements of the flow field. The model grid division is shown in Figure 4. According to the principle of grid independence testing, the final number of grids was determined to be 3.32 million. Simulation was made on workstation (Intel (R) Core (TM) i9-10 900 CPU @ 2.80 GH processor; 64.0 GB of memory), and the grid generation time was approximately 5 min.

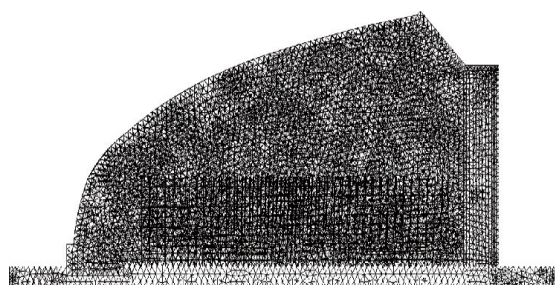


Figure 4 Grid division diagram

2.2.2 Model simplifications

1) During the experiment, the greenhouse's tool room did not participate in indoor heat and humidity exchange, and the door connecting the tool room to the indoor was closed, so the physical model ignored the tool room and the door;

2) The east and west sides of the soil and the bottom layer were set as insulation;

3) The gas phase consisted only of a binary ideal gas mixture of dry air and water vapor;

4) Ignoring soil moisture evaporation and condensation, and considering the indoor humidity affects were crop transpiration;

5) Neglecting the impact of greenhouse cold air infiltration;

6) Neglecting the mutual influence in the heat and moisture transfer process, namely the Soret effect and Dofour effect.

2.2.3 Governing equations

When the CSG was in a natural ventilated (outdoor wind speed less than 2 m/s) or closed state, the fluid generates buoyancy due to density changes, which was represented by the following equation:

$$\beta = -\frac{1}{\rho} \left(\frac{\partial \rho}{\partial T} \right)_p = \frac{\rho_0 - \rho}{\rho(T - T_0)} \quad (1)$$

$$\rho = \rho_0 [1 - \beta(T - T_0)] \quad (2)$$

where, β is the coefficient of thermal expansion; T_0 is the reference temperature, °C; ρ_0 is the fluid density, kg/m³. When $T - T_0 < 15^\circ\text{C}$, the Boussinesq hypothesis was applicable.

The mass and heat transfer process in CSG can be described by the general control Equation (3):

$$\frac{\partial(\rho\varphi)}{\partial t} + \operatorname{div}(\rho v\varphi) = \operatorname{div}(\Gamma \operatorname{grad}\varphi) + S_\varphi \quad (3)$$

where, φ is a dimensionless transfer quantity, namely momentum, mass (mass fraction of air and water vapor), energy; t is the time, s; Γ is the generalized diffusion coefficient, m²/s; S_φ is the source item, W/m³.

To simulate the impact of solar radiation on the temperature and humidity field inside the greenhouse, the solar tracking model and discrete ordinates (DO) radiation were activated together, and a solar calculator was used to set the simulation date and the longitude and latitude of the area where the greenhouse was located. In addition, the sunshine clarity index was adjusted according to the measured solar radiant intensity^[19]. The radiation equation is shown in Equation (4):

$$\nabla \cdot (I(\vec{r}, \vec{s}) \vec{s}) + (\alpha + \sigma_s) I(\vec{r}, \vec{s}) = an^2 \frac{\sigma T^4}{\pi} + \frac{\sigma_s}{4\pi} \int_0^{4\pi} I(\vec{r}, \vec{s}') \Phi(\vec{s}' \cdot \vec{s}) d\Omega' \quad (4)$$

where, \vec{r} is the position vector; \vec{s} is the direction vector; \vec{s}' is the scattering direction vector; α is the absorption coefficient; n is the refraction coefficient; σ_s is the scattering coefficient; σ is the Stephen Boltzmann constant, $5.672 \times 10^{-8} \text{ W}/(\text{m}^2 \cdot \text{K}^4)$; I is the radiant intensity, W/m^2 ; Φ is the phase function; Ω' is the solid angle of radiation, (°).

The study considered tomato crops as porous media, satisfying Darcy-Forchheimer law^[20], and the equation is as follows:

$$S_\varphi = - \left(\frac{\mu}{K_p} v + \frac{C_F}{\sqrt{K_p}} \rho v^2 \right) \quad (5)$$

$$C_1 = \frac{1}{K_p} \quad (6)$$

$$C_2 = \frac{2C_F}{K_p^{0.5}} \quad (7)$$

where, K_p is the penetration rate of tomato crops, m^{-2} ; C_F is the nonlinear momentum loss coefficient of tomato crops; C_1 is the viscous resistance coefficient, m^{-2} ; C_2 is the inertial drag coefficient, m^{-1} .

The resistance effect generated by crops can usually be represented by Equation (8)^[21]:

$$S_\varphi = -\rho LADC_D v^2 \quad (8)$$

where, LAD is the leaf area density, m^2/m^3 ; C_D is the resistance coefficient of tomato crops, 0.32.

Ignoring the first order part of the source term of Equation (5), only the second order part was considered. At the same time, by combining Equation (8), the relationship between the nonlinear momentum loss coefficient and permeability was obtained as follows:

$$S_\varphi = \frac{C_F}{\sqrt{K_p}} = \text{LADC}_D \quad (9)$$

K_p can be calculated based on empirical equation^[22]:

$$K_p = \frac{d_p^2 \varepsilon}{180(1 - \varepsilon)^2} \quad (10)$$

where, d_p is the characteristic size of the crop, m; ε is the porosity of the crop canopy.

Measure and calculate the porosity of tomato canopy as 0.98, and the characteristic size of tomato crops is taken as 0.15 m. The calculated values of K_p and C_F are 0.306 and 0.242, respectively. Then C_1 and C_2 can be calculated as 3.268 and 0.88, respectively.

Neglect the impact of substrate and soil evaporation on indoor water vapor content, without considering the heat storage effect of the canopy^[23]. The exchange of sensible and latent heat between crops and indoor air, as well as the transfer of water vapor, satisfied the following equation:

$$G_a + Q_s + Q_l = 0 \quad (11)$$

$$Q_s = 2\text{LAD} \frac{\rho_a C_p}{r_a} (T_1 - T_a) \quad (12)$$

$$Q_l = \text{LAD} \frac{L_w \rho_a}{r_s + r_a} (w_1 - w_a) \quad (13)$$

where, G_a is the net radiation density absorbed by the canopy, W/m^3 ; Q_s is the sensible heat flux density between leaves and air, W/m^3 ; Q_l is the latent heat flux density related to crop transpiration, W/m^3 ; C_p is the specific heat of air at constant pressure, $\text{J}/\text{kg} \cdot \text{K}$; r_a is the aerodynamic resistance of the blade, s/m ; T_1 and T_a are the temperature of the blade and air, °C, respectively; L_w is the heat absorbed by the latent heat of water evaporation; w_1 and w_a are the absolute humidity of the leaves and air, $\text{kg}_{\text{water}}/\text{kg}_{\text{air}}$; r_s is the stomatal resistance of the leaves, s/m .

The component transport equation is used to simulate the interaction between various components in the mixture, describing the diffusion process of indoor water vapor with air flow. The equation is as follows:

$$\frac{\partial(\rho c_s)}{\partial t} + \operatorname{div}(\rho v c_s) = \operatorname{div}(D_s \operatorname{grad}(\rho c_s)) + S_s \quad (14)$$

where, s is a component variable; ρc_s is the mass concentration of component s , kg/m^3 ; c_s is the volume concentration of component s ; D_s is the diffusion coefficient of component s , m^2/s ; S_s is the generation rate of component s , $\text{kg}/\text{m}^3 \cdot \text{s}$.

2.2.4 Initial and boundary conditions

To solve the problem of dynamic changes and uneven distribution of indoor environment and improve model accuracy, a general form of binary fitting function (binary quadratic polynomial) was constructed. The parameter values were obtained through actual measurements, and the fitting function was loaded into the CFD model in UDF format for model initialization and boundary condition setting. The general form of the fitting function is as follows:

$$F = Ax^2y^2 + Bx^2y + Cxy^2 + Dx^2 + Ey^2 + Fxy + Gx + Hy + I \quad (15)$$

Outdoor wind speed, air temperature and humidity are highly correlated with time changes. Considering the impact of outdoor environment on indoor environment, a regression equation for the temporal variation of outdoor environmental factors was established and loaded onto the boundary conditions of the model. At the same time, the temperature of the outer surface of the back wall and the north-south boundary of the soil fluctuated significantly due to factors such as solar radiation and wind speed. A binary fitting function of temperature with respect to height and time was constructed, and the specific parameters are listed in Table 2. The dependent variable F is the temperature of the external surface of the back wall and the external surface of the soil, the independent variable x is the simulation duration (0-3600 s), and the independent variable y is the coordinate value along the height direction, so as to realize the process simulation of the dynamic changes of the external surface of the soil, the external surface of the back wall and the outdoor environment of the CSG.

Table 2 Parameter values in boundary condition fitting functions

| $F/^\circ\text{C}$ | A | B | C | D | E | F | G | H | I |
|---|-----|-----|-----|-----|-----|-----|-----|-----|-----|
| Outer surface temperature of back wall | | | | | | | | | |
| 0.000 0.000 0.000 0.245 0.000 0.001 0.215 0.000 -5.153 | | | | | | | | | |
| Outer surface of northern marginal soil | | | | | | | | | |
| 0.000 0.0040 0.000 -23.111 0.000 0.002 -25.879 0.000 -6.338 | | | | | | | | | |
| Outer surface of southern marginal soil | | | | | | | | | |
| 0.000 0.006 0.000 -5.1140 0.000 0.0040 -12.000 0.001 -1.231 | | | | | | | | | |

2.2.5 Solving methodology

Take 9:00 am as the initial time of simulation, and simulate the indoor temperature and humidity distribution after one hour. Use ANSYS Fluent as the model simulation solver and the standard $k-\epsilon$ turbulence model, select the standard wall function as the wall function, and verify that the dimensionless wall distance y^+ range in each region of the model is 10-150, which met the calculation requirements of the turbulence model^[24]. Due to the low airflow velocity within the crop canopy, a laminar flow model was used for calculation within the crop canopy area.

2.3 Determination of building parameter combination

Orthogonal experiment is an efficient experimental design method that studies different factors and levels. By selecting representative combinations of levels from comprehensive experiments, it aims to reduce the number of experiments while reflecting the objective laws of things, and has high computational efficiency^[25].

2.3.1 Factors and level selection

During the selection process of orthogonal experimental factors, it is necessary to analyze the actual problems and ultimately select the main factors. Select ridge height, back wall height, and back roof horizontal projection as the main optimization parameters, with a difference of 0.4 m between each level. The experimental factor levels are listed in Table 3.

Table 3 Factor and level table

| Level | A1 | | | A2 | | | A3 | | |
|-------|----------------|--------------------|-----------------------------------|----------------|--------------------|-----------------------------------|----------------|--------------------|-----------------------------------|
| | Ridge height/m | Back wall height/m | Back roof horizontal projection/m | Ridge height/m | Back wall height/m | Back roof horizontal projection/m | Ridge height/m | Back wall height/m | Back roof horizontal projection/m |
| 1 | 4.52 | 3.2 | 0.9 | | | | | | |
| 2 | 4.92 | 3.6 | 1.3 | | | | | | |
| 3 | 5.32 | 4.0 | 1.7 | | | | | | |
| 4.0 | 5.72 | 4.4 | 2.1 | | | | | | |

2.3.2 Orthogonal test scheme

The orthogonal test was conducted with 3 factors and 4 levels. The $L_{16}(4^5)$ standard orthogonal table (Table 4) and the actual building parameters were selected in the final orthogonal test.

Table 4 Orthogonal test scheme

| No. | Test plan | A1(Ridge height/m) | A2(Back wall height/m) | A3(Back roof horizontal projection/m) |
|-----|--|--------------------|------------------------|---------------------------------------|
| 1 | A ₁ B ₁ C ₁ | 4.52 | 3.2 | 0.9 |
| 2 | A ₁ B ₂ C ₂ | 4.52 | 3.6 | 1.3 |
| 3 | A ₁ B ₃ C ₃ | 4.52 | 4.0 | 1.7 |
| 4 | A ₁ B ₄ C ₄ | 4.52 | 4.4 | 2.1 |
| 5 | A ₂ B ₁ C ₂ | 4.92 | 3.2 | 1.3 |
| 6 | A ₂ B ₂ C ₁ | 4.92 | 3.6 | 0.9 |
| 7 | A ₂ B ₃ C ₄ | 4.92 | 4.0 | 2.1 |
| 8 | A ₂ B ₄ C ₃ | 4.92 | 4.4 | 1.7 |
| 9 | A ₃ B ₁ C ₃ | 5.32 | 3.2 | 1.7 |
| 10 | A ₃ B ₂ C ₄ | 5.32 | 3.6 | 2.1 |
| 11 | A ₃ B ₃ C ₁ | 5.32 | 4.0 | 0.9 |
| 12 | A ₃ B ₄ C ₂ | 5.32 | 4.4 | 1.3 |
| 13 | A ₄ B ₁ C ₄ | 5.72 | 3.2 | 2.1 |
| 14 | A ₄ B ₂ C ₃ | 5.72 | 3.6 | 1.7 |
| 15 | A ₄ B ₃ C ₂ | 5.72 | 4.0 | 1.3 |
| 16 | A ₄ B ₄ C ₁ | 5.72 | 4.4 | 0.9 |

2.4 Entropy weight method and comprehensive evaluation index of thermal and humidity environment

2.4.1 Thermal and humidity environment evaluation index

1) Temperature rise rate

The rate of temperature rise can reflect the variation of indoor temperature over time, and the calculation equation was as follows:

$$K_{\text{air}} = \frac{T_2 - T_1}{\Delta t} = \frac{\Delta T}{\Delta t} \quad (16)$$

where, K_{air} is the air temperature rise rate, $^\circ\text{C}/\text{min}$; T_2 is the final determination of average temperature of indoor air, $^\circ\text{C}$; T_1 is the initial measurement of average temperature of indoor air, $^\circ\text{C}$; Δt is the time difference between T_1 and T_2 , min.

2) Temperature and humidity uneven coefficient

In order to accurately reflect the uneven degree of temperature and humidity distribution in CSG, the uneven coefficient of temperature and humidity was introduced, and its calculation equation was as follows:

$$S_T = \frac{\sigma_T}{\bar{T}} \quad (17)$$

$$S_R = \frac{\sigma_R}{\bar{R}} \quad (18)$$

where, S_T is the air temperature uneven coefficient; S_R is the humidity uneven coefficient; \bar{T} is the average indoor air temperature, $^\circ\text{C}$; \bar{R} is the average indoor air humidity, %; σ_T is the temperature root mean square error, $^\circ\text{C}$; σ_R is the humidity root mean square error, %.

$$\sigma_T = \sqrt{\frac{\sum (T_i - \bar{T})^2}{n_{\text{air}}}} \quad (19)$$

$$\sigma_R = \sqrt{\frac{\sum (R_i - \bar{R})^2}{n_{\text{air}}}} \quad (20)$$

where, T_i is the indoor air measurement point temperature, $^\circ\text{C}$; R_i is the indoor air measurement point humidity, %; n_{air} is the number of indoor air temperature and humidity measurement points.

3) Average temperature and humidity

To accurately reflect the overall situation of temperature and humidity in CSG, the average temperature and humidity index was introduced, and the calculation equation is as follows:

$$\bar{T} = \frac{\sum_{i=1}^n T_i}{n_{\text{air}}} \quad (21)$$

$$\bar{R} = \frac{\sum_{i=1}^n R_i}{n_{\text{air}}} \quad (22)$$

2.4.2 Entropy weight method and comprehensive evaluation index establishment

The entropy weight method, as a commonly used comprehensive evaluation method, judges the weight of each indicator based on the differences between them and the degree of dispersion. Generally, the greater the degree of dispersion of an indicator, the more information it contains, as its weight setting is calculated from the data itself and is not influenced by subjective factors of decision-makers.

The steps for determining the comprehensive indicators of greenhouse thermal and humidity environment using entropy weight method were as follows:

1) Construct an initial thermal and humidity environment comprehensive index matrix

Assuming there are m_0 sample values for evaluation objects and n_0 thermal and humidity environment evaluation indicators, construct the initial thermal and humidity environment comprehensive indicator matrix A as follows:

$$A = (a_{ij})_{m_0 \times n_0}, (i = 1, 2, \dots, m_0; j = 1, 2, \dots, n_0) \quad (23)$$

where, a_{ij} is the sample value of the i th evaluation object under the j th thermal and humidity environmental indicator.

2) Standardized processing of indicators

In order to eliminate dimensional differences between different evaluation indicators, the initial thermal and humidity environment comprehensive indicator matrix was normalized.

For positive indicators, the standardization process is:

$$x_{ij} = \frac{a_{ij} - a_j^{\min}}{a_j^{\max} - a_j^{\min}} \quad (24)$$

For negative indicators, the standardization process is:

$$x_{ij} = \frac{a_j^{\max} - a_{ij}}{a_j^{\max} - a_j^{\min}} \quad (25)$$

For interval type indicators, set the optimal interval as $[e, f]$, which was the unbearable lower limit and the unbearable upper limit. The standardization process is as follows:

$$x_{ij} = \begin{cases} 1 - \frac{(e - a_{ij})}{(e - a_j^0)}, & a_{ij} \in [a_j^0, e] \\ 1, & a_{ij} \in [e, f] \\ 1 - \frac{(a_{ij} - f)}{(a_j^* - f)}, & a_{ij} \in (f, a_j^*) \\ 0, & \text{else} \end{cases} \quad (26)$$

where, x_{ij} is the standard sample value of the i th evaluation object under the j th thermal and humidity environment indicator; a_j^{\max} is the maximum value of the j th thermal and humidity environment indicator; a_j^{\min} is the minimum value of the j th thermal and humidity

environment indicator.

3) Calculate the specific gravity matrix

The proportion matrix of comprehensive index of thermal and humidity environment was $P = (p_{ij})_{m_0 \times n_0}$, p_{ij} represented the proportion of sample value of the i th assessment object under the j th thermal and humidity environment index of CSG in this index, as shown below:

$$p_{ij} = \frac{x_{ij}}{\sum_{i=1}^{m_0} x_{ij}}, (i = 1, 2, \dots, m_0; j = 1, 2, \dots, n_0) \quad (27)$$

4) Calculation of information entropy matrix for comprehensive indicators of thermal and humidity environment

The information entropy matrix of the thermal and humidity environment comprehensive index is $E = (e_j)$, e_j represented the information entropy of the j th thermal and humidity environment index, as shown below:

$$e_j = \frac{1}{\ln m_0} \sum_{i=1}^{m_0} p_{ij} I_{ij}, (j = 1, 2, \dots, n_0) \quad (28)$$

where, $I_{ij} = -\ln p_{ij}$ represents the information content of the i th evaluation object under the j th thermal and humidity environmental indicator of the CSG. The larger the proportion of the thermal and humidity environmental indicator value p_{ij} , the smaller the uncertainty of the indicator itself, and the smaller the information content it contained. The maximum value of $\sum_{i=1}^{m_0} p_{ij} I_{ij}$ is $-\ln m_0$, so when calculating the information entropy e_j , divide by the constant $\ln m_0$ to ensure $e_j \in [0, 1]$.

5) Calculate weight matrix

The weight matrix of comprehensive index of thermal and humidity environment is $W = (w_j)$, w_j represents the weight of the j th thermal and humidity environment index of CSG, as shown below:

$$w_j = \frac{d_j}{\sum_{j=1}^n d_j}, (j = 1, 2, \dots, n_0) \quad (29)$$

where, $d_j = 1 - e_j$ represents the information utility value of the j th thermal and humidity environmental indicator in the CSG. When the information entropy e_j of the thermal and humidity environment index was larger, the amount of information carried was smaller, and the information utility value d_j was smaller.

6) Determine comprehensive evaluation indicators

In order to facilitate the subsequent selection of optimal building parameters, the comprehensive evaluation index for the thermal and humidity environment of CSG is specified as extremely large data, that is, the larger the data value, the better the indoor thermal and humidity environment. Five indicators, namely air temperature rise rate, uneven coefficient of air temperature and humidity, and average temperature and humidity, were selected as the evaluation indicators for the thermal and humidity environment of CSG. The 16 sets of building parameter simulation results obtained from the orthogonal experimental plan were used as the evaluation objects. Based on the linear weighting principle, the standard values of each indicator are multiplied by the corresponding weight coefficients and linearly added to obtain the comprehensive evaluation indicators.

$$D_i = w_1 x_1 + w_2 x_2 + \dots + w_n x_{n_0} = \sum_{j=1}^{n_0} w_j x_{ij}, (i = 1, 2, \dots, m_0) \quad (30)$$

where, D_i is the comprehensive evaluation index for the thermal and humidity environment.

3 Results and discussion

3.1 Numerical model validation

Considering the crop as a porous medium, and the latent and sensible heat of the crop were loaded into the crop area in the form of source terms. Combined with the component transport equation, this study simulated the changes in the indoor thermal and humidity environment after 1 h and the simulation results were compared with the measured data. In order to evaluate the reliability of the numerical model, root mean square error (RMSE) and mean absolute error (MAE) were used to evaluate the fitting degree between the simulated value and the measured value. The RMSE and MAE of soil temperature, air temperature and humidity, and back wall temperature were calculated, with the highest RMSE of temperature and relative humidity being 1.69°C and 5.66%, and the highest MAE of temperature and relative humidity being 1.34°C and 4.65%, respectively. The error values were all within the acceptable range of simulation, proving the effectiveness of the model, as listed in Table 5.

Table 5 Numerical model verification results

| Soil temperature | | Back wall temperature | | Air temperature | | Air humidity | |
|------------------|--------|-----------------------|--------|-----------------|--------|--------------|-------|
| RMSE | MAE | RMSE | MAE | RMSE | MAE | RMSE | MAE |
| 1.22°C | 0.66°C | 1.54°C | 0.96°C | 1.69°C | 1.34°C | 5.66% | 4.65% |

3.2 Optimization of building parameters

3.2.1 Entropy weight method to determine weight coefficient

Numerical simulation was used to calculate the thermal and humidity environment simulation results of a CSG under 16 different building parameters, and the thermal and humidity environment evaluation indicators were calculated. Considering that the temperature rise rate was an extremely large indicator, the temperature and humidity uneven coefficient was an extremely small indicator, and the average temperature and humidity were interval type indicators, the initial results of the thermal and humidity environment evaluation obtained will be standardized and forward processed. The optimal temperature range for tomatoes was set at 20°C-25°C, with upper and lower limits of 32.2°C and 18.3°C, respectively. During the experiment, tomatoes were in the fruit ripening stage, and the optimal relative humidity range was set at 55%-65%. The upper and lower limits of relative humidity were set at 40% and 90%, respectively. The standardized calculation results are listed in Table 6.

According to the steps of entropy weight method, the information entropy, information utility value and weight calculation results of thermal and humidity environment indicators are listed in Table 7. The size of the weight reflects the degree of influence of this parameter. The weights of different thermal and humidity environmental indicators were in descending order: humidity uneven coefficient>temperature rise rate>temperature uneven coefficient>average temperature>average humidity.

3.2.2 Comprehensive evaluation index calculation

Substitute the weight of thermal and humidity environmental indicators into Equation (30) to obtain a comprehensive evaluation index:

$$D_i = 0.343x_1 + 0.219x_2 + 0.417x_3 + 0.018x_4 + 0.003x_5 \quad (31)$$

where, x_1 is the standardized sample value of temperature rise rate; x_2 is the standardized sample value of temperature uneven

coefficient; x_3 is the standardized sample value of humidity uneven coefficient; x_4 is the average temperature standardized sample value; and x_5 is the average humidity standardized sample value.

Substitute the standardized results of greenhouse thermal and humidity environment evaluation indicators into Equation (31) and linearly add them to obtain the comprehensive evaluation index scores of different building parameter combinations, as shown in Figure 5.

Table 6 Standardization results of thermal and humidity environment evaluation indicators

| No. | Test plan | Temperature rise rate | Temperature uneven coefficient | Humidity uneven coefficient | Average temperature | Average humidity |
|-----|--|-----------------------|--------------------------------|-----------------------------|---------------------|------------------|
| 1 | A ₁ B ₁ C ₁ | 0.889 | 0.693 | 0.243 | 0.23 | 0.97 |
| 2 | A ₁ B ₂ C ₂ | 0.723 | 0.179 | 0.457 | 0.25 | 1.00 |
| 3 | A ₁ B ₃ C ₃ | 0.707 | 0.604 | 0.235 | 0.25 | 1.00 |
| 4 | A ₁ B ₄ C ₄ | 0.770 | 0.685 | 0.392 | 0.24 | 1.00 |
| 5 | A ₂ B ₁ C ₂ | 1.000 | 0.751 | 0.371 | 0.21 | 0.90 |
| 6 | A ₂ B ₂ C ₁ | 0.826 | 0.639 | 0.207 | 0.24 | 0.92 |
| 7 | A ₂ B ₃ C ₄ | 0.549 | 0.504 | 0.000 | 0.28 | 0.99 |
| 8 | A ₂ B ₄ C ₃ | 0.368 | 0.580 | 0.212 | 0.30 | 1.00 |
| 9 | A ₃ B ₁ C ₃ | 0.823 | 0.944 | 0.832 | 0.24 | 0.86 |
| 10 | A ₃ B ₂ C ₄ | 0.097 | 0.227 | 0.193 | 0.34 | 0.97 |
| 11 | A ₃ B ₃ C ₁ | 0.476 | 0.631 | 0.213 | 0.29 | 0.92 |
| 12 | A ₃ B ₄ C ₂ | 0.151 | 0.564 | 0.190 | 0.31 | 0.93 |
| 13 | A ₄ B ₁ C ₄ | 0.597 | 1.000 | 1.000 | 0.27 | 0.82 |
| 14 | A ₄ B ₂ C ₃ | 0.523 | 0.953 | 0.900 | 0.28 | 0.83 |
| 15 | A ₄ B ₃ C ₂ | 0.086 | 0.853 | 0.746 | 0.34 | 0.91 |
| 16 | A ₄ B ₄ C ₁ | 0.000 | 0.000 | 0.239 | 0.34 | 0.91 |

Table 7 Information entropy, information utility value and weight of thermal and humidity environment evaluation indicators

| Parameters | Temperature rise rate | Temperature uneven coefficient | Humidity uneven coefficient | Average temperature | Average humidity |
|---------------------------|-----------------------|--------------------------------|-----------------------------|---------------------|------------------|
| Information entropy | 0.924 | 0.951 | 0.907 | 0.996 | 0.999 |
| Information utility value | 0.076 | 0.049 | 0.093 | 0.004 | 0.001 |
| weight | 0.343 | 0.219 | 0.417 | 0.018 | 0.003 |

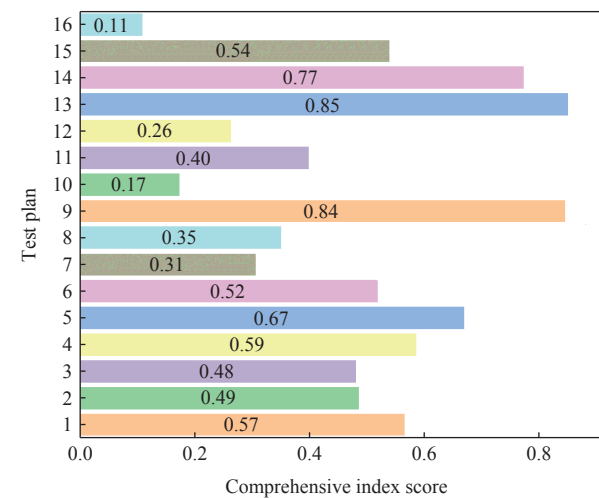


Figure 5 Score of comprehensive evaluation indicators for thermal and humidity environment under different combinations of building parameters

From Figure 5, it can be seen that the combination of building parameters $A_4B_1C_4$ (ridge height of 5.72 m, back wall height of 3.20 m, and horizontal projection of back roof of 2.10 m) had the highest comprehensive evaluation index score for the thermal and humidity environment of the greenhouse, indicating that the greenhouse had the best thermal and humidity environment under this building parameter. On the contrary, the comprehensive evaluation index score for the thermal and humidity environment of the CSG building parameter combination $A_4B_4C_1$ (ridge height of 5.72 m, back wall height of 4.40 m, and horizontal projection of the back roof of 0.90 m) was the lowest, indicating that the thermal and humidity environment of the greenhouse was the worst under this building parameter.

4 Conclusions

A building parameter optimization method was proposed based on CFD simulation and entropy weight method. A thermal and humidity environment model under the coupling effect of soil crop back wall in a Chinese solar greenhouse (CSG) was constructed, and its reliability was verified through practical testing. With analysis and determination on the main building parameters of a CSG, the air temperature rise rate, air temperature and humidity uneven coefficient, and average air temperature and humidity were selected as the evaluation indicators for the thermal and humidity environment. Combining numerical simulation, a 3-factor and 4-level orthogonal experiment was conducted to obtain the calculation results of various indicators of the thermal and humidity environment under different building parameter combinations. The weight coefficients were assigned to each indicator by using the entropy weight method, and finally to obtain the comprehensive evaluation indicators of the greenhouse thermal and humidity environment. The results showed that the optimal combination of building parameters for the greenhouse was $A_4B_1C_4$, with a ridge height of 5.72 m, a back wall height of 3.20 m, and a horizontal projection of 2.10 m on the back roof.

Acknowledgements

The authors would like to acknowledge the support provided by Hebei Province Key Research and Development Program (Grant No. 22327214D) and Independent Research and Development Plan of Academy of Agricultural Planning and Engineering, Ministry of Agriculture and Rural Affairs (Grant No. SP202101).

[References]

- [1] Li T L. Theory and practice of vegetable cultivation in solar greenhouse. Beijing: China Agriculture Press, 2013. (in Chinese)
- [2] Zhang R, Liu Y C, Zhu D L, Zhang X M, Ge M S, Cai Y H. Optimal design for solar greenhouses based on canopy height. *Journal of Building Engineering*, 2022; 53: 104473.
- [3] Liu X G, Wu X Y, Xia T Y, Fan Z L, Shi W B, Li Y M, et al. New insights of designing thermal insulation and heat storage of Chinese solar greenhouse in high latitudes and cold regions. *Energy*, 2022; 242: 122953.
- [4] He F, Tian J, Wang L, Hou Y, Qi F, Zhang Y P, et al. Effects of different root zone heating systems on the microclimate and crop development in solar greenhouses. *Int J Agric & Biol Eng*, 2022; 15(6): 67–72.
- [5] Tong G H, Christopher D M, Li T L, Wang T L. Passive solar energy utilization: A review of cross-section building parameter selection for Chinese solar greenhouses. *Renewable and Sustainable Energy Reviews*, 2013; 26: 540–548.
- [6] NY/T 3223-2018. Code for design of Chinese solar greenhouse. Chinese Standard, 2018. (in Chinese)
- [7] Cao Y F, Jing H W, Zhao S M, Zou Z R, Bao E C. Optimization of back roof projection width and northern wall height in Chinese solar greenhouse. *Transactions of the CSAE*, 2017; 33(7): 183–189. (in Chinese)
- [8] Tong X J, Sun Z P, Sigrimis N, Li T L. Energy sustainability performance of a sliding cover solar greenhouse: Solar energy capture aspects. *Biosystem Engineering*, 2018; 176: 88–102.
- [9] Yang F G, Chen C, Ma C W, Li Y, Han F T, Li Y R, et al. Discussion on the principle of selecting spatial characteristic parameters of solar greenhouse morphology with low energy consumption. *Xinjiang Agricultural Sciences*, 2018; 55(3): 535–547. (in Chinese)
- [10] Zhang G X, Fu Z T, Yang M S, Liu X X, Dong Y H, Li X X. Nonlinear simulation for coupling modeling of air humidity and vent opening in Chinese solar greenhouse based on CFD. *Computers and Electronics in Agriculture*, 2019; 162: 337–347.
- [11] He X L, Wang J, Guo S R, Zhang J, Wei B, Sun J, et al. Ventilation optimization of solar greenhouse with removable back walls based on CFD. *Computers and Electronics in Agriculture*, 2018; 149: 16–25.
- [12] Zhang X, Wang H L, Zou Z R, Wang S J. CFD and weighted entropy based simulation and optimisation of Chinese solar greenhouse temperature distribution. *Biosystem Engineering*, 2016; 142: 12–26.
- [13] Tong G H, Christopher D M, Li B M. Numerical modelling of temperature variations in a Chinese solar greenhouse. *Computers and Electronics in Agriculture*, 2009; 68: 129–139.
- [14] Liu X G, Li H, Li Y M, Yue X, Tian S B, Li T L. Effect of internal surface structure of the north wall on Chinese solar greenhouse thermal microclimate based on computational fluid dynamics. *Plos One*, 2020; 15(4): e0231316.
- [15] Li Y M, Liu X G, Qi F S, Wang L, Li T L. Numerical investigation of the north wall passive thermal performance for Chinese solar greenhouse. *Thermal Science*, 2020; 24(6A): 3465–3476.
- [16] Wu X Y, Liu X G, Yue X, Xu H, Li T L, Li Y M. Effect of the ridge position ratio on the thermal environment of the Chinese solar greenhouse. *Royal Society Open Science*, 2017; 8: 1–16.
- [17] Tong G H, Christopher D M, Zhang G Q. New insights on span selection for Chinese solar greenhouses using CFD Analyses. *Computers and Electronics in Agriculture*, 2018; 149: 3–15.
- [18] Li W Y. Simulation study of different structure parameters of solar greenhouse based on computational fluid dynamics in the winter. Shenyang Agricultural University, 2020. (in Chinese)
- [19] Li H, Ji D, Hu X, Xie T, Song W T, Tian S B. Comprehensive evaluation of combining CFD simulation and entropy weight to predict natural ventilation strategy in a sliding cover solar greenhouse. *Int J Agric & Biol Eng*, 2021; 14(6): 213–221.
- [20] Boulard T, Wang S. Experimental and numerical studies on the heterogeneity of crop transpiration in a plastic tunnel. *Computers and Electronics in Agriculture*, 2002; 34(1-3): 173–190.
- [21] Wilson J D. Numerical studies of flow through a windbreak. *Journal of Wind Engineering and Industrial Aerodynamics*, 1985; 21(2): 119–154.
- [22] Nield D A, Bejan A. Convection in porous media. New York: Springer, 2006.
- [23] Stanghellini C. Transpiration of greenhouse crops: an aid to climate management. Doctoral thesis, Wageningen University, 1987.
- [24] Blocken B, Stathopoulos T, Carmeliet J. CFD simulation of the atmospheric boundary layer: wall function problems. *Atmospheric Environment*, 2007; 41(2): 238–252.
- [25] Liu F D, Li Y, Liu Y. The application of single index test and orthogonal test in the analysis of parameter sensitivity. *Journal of Water Resources and Architectural Engineering*, 2015; 13(6): 85–88, 177. (in Chinese)